

POPULATION SYNTHESIS OF GALACTIC BE-STAR BINARIES WITH A HELIUM-STAR COMPANION

YONG SHAO^{1,2} AND XIANG-DONG LI^{1,2}

¹Department of Astronomy, Nanjing University, Nanjing 210046, People's Republic of China; shaoyong@nju.edu.cn and
²Key laboratory of Modern Astronomy and Astrophysics (Nanjing University), Ministry of Education, Nanjing 210046, People's Republic of China; lixd@nju.edu.cn

Draft version December 14, 2020

ABSTRACT

LB-1 was originally suggested to harbour a very massive ($\sim 70M_{\odot}$) black hole, but was recently suggested to be a post-mass transfer binary containing a Be star and a helium (He) star. In this paper, we use the binary population synthesis method to simulate the potential population of the Be–He binaries in the Milky Way. Mass transfer process during the progenitor binary evolution plays a vital role in determining the possible properties of the Be–He binary population. By constructing a range of physical models with significantly different mass-transfer efficiencies, we obtain the predicted distributions at the current epoch of the component masses and the orbital periods for the Be–He binaries. In particular, we show that, LB-1 very likely has evolved through non-conservative mass transfer if it is indeed a Be–He system. We estimate that there are more than 10^3 Be–He binaries with V-band apparent magnitudes brighter than LB-1.

Subject headings: binaries: general – binaries: close – stars: evolution

1. INTRODUCTION

Liu et al. (2019) reported the discovery of a unique binary system LB-1 that may harbour a $\sim 70M_{\odot}$ black hole with a B-type star in a ~ 79 day orbit. The formation of such a massive black hole would drastically challenge current stellar evolution theories, since it is not expected to be created in a Galactic high-metallicity environment due to strong stellar winds (e.g., Belczynski et al. 2010) and pair-instability supernovae (e.g., Farmer et al. 2019). This has led to some exotic scenarios for the formation of this source (Groh et al. 2019; Belczynski et al. 2020). On the other hand, other groups (e.g., Abdul-Masih et al. 2020; El-Badry & Quataert 2020; Eldridge et al. 2020; Irngang et al. 2020; Simón-Díaz et al. 2020) suggest that LB-1 may actually host a normal stellar-mass black hole. Until now, the nature of LB-1 is still under debate (Liu et al. 2020). More recently, Shenar et al. (2020) argued that LB-1 does not contain a compact star but instead a post-mass transfer binary comprising of a $\sim 7M_{\odot}$ Be star and a $\sim 1.5M_{\odot}$ stripped star.

The formation of Be stars is not fully understood, but there is a consensus that they are rapid rotators with the equatorial velocities near their Keplerian limits (e.g., Porter & Rivinius 2003). It has been proposed that three main mechanisms are responsible for the rapid rotation of Be stars: (1) they were born as rapid rotators by inheriting the angular momentum from their parental molecular clouds (see however, Huang et al. 2010); (2) angular momentum transfer from the core to the envelope during the main-sequence evolution (e.g., Ekström et al. 2008; Hastings et al. 2020); (3) they are the mass gainers or the stellar mergers as a consequence of binary interaction (e.g., Rappaport & van den Heuvel 1982; Pols et al. 1991; Shao & Li 2014). Investigations on the observed sample of Be stars suggest that a large majority of them have formed via binary mass transfer (McSwain & Gies 2005; Bodensteiner et al. 2020a).

Observations show that massive stars of spectral types O and B are born predominately in binary and multi-

ple systems (Sana et al. 2012; Kobulnicky 2014; Moe & Di Stefano 2017). The majority of them will interact with a binary companion via mass transfer, which significantly changes the evolutionary paths of both stars and the orbital parameters of the binary system. A fraction of binary systems are expected to evolve through a stable Roche-lobe overflow phase, during which the primary star loses most of its hydrogen envelope while the secondary star is rejuvenated and spun up due to mass accretion (Hurley et al. 2002). After the mass transfer, the primary evolves to be a stripped helium (He) star (also referred as hot subdwarf star or Wolf-Rayet star) and the secondary appears to be a rapidly rotating Be star, leading to the formation of a Be–He binary (Pols et al. 1991; Shao & Li 2014; Langer et al. 2020). The subsequent evolution of such systems is likely to become Be/X-ray binaries if the He stars are massive enough to quickly evolve into compact stars. Population synthesis studies indicate that the number of Galactic Be–He binaries is of the order 10^5 , which is comparable with that of Be–white-dwarf systems and about two orders of magnitude more than that of both Be–neutron-star and Be–black-hole systems (Shao & Li 2014). In this paper, we focus on the detailed properties of Galactic Be–He binaries and the formation of the peculiar system LB-1.

To date, there are several Be–He systems confirmed in the Milky Way (Wang et al. 2018), e.g. φ Persei (Mourard et al. 2015), FY CMa (Peters et al. 2008), 59 Cyg (Peters et al. 2013), 60 Cyg (Wang et al. 2017), HR 2142 (Peters et al. 2016), and *O* Puppis (Koubský et al. 2012). More recently, HR 6819 was also suggested to be a Be–He binary (Bodensteiner et al. 2020b) rather than a triple system with a black hole (Rivinius et al. 2020). The orbital periods of these Be–He binaries vary in the range of $\sim 30 - 150$ days. All in the observed sample host a He star with mass around $1M_{\odot}$. The masses of the Be star are distributed in the range of $\sim 6 - 12M_{\odot}$.

One of the most important parameters that can significantly influence the properties of Be–He systems is the

mass-transfer efficiency (i.e. the fraction of the accreted matter by the secondary star among all the transferred matter). Based on the parameters of the well-studied source φ Persei, Schootemeijer et al. (2018) evolved an extensive grid of binary systems to reproduce this binary by varying the mass-transfer efficiency in a range of 0.25 – 1.0. They concluded that this system must have experienced a near-conservative mass transfer stage, which is consistent with earlier studies of Vanbeveren et al. (1998) and Pols (2007). It has been suggested that, however, the evolution of massive binaries can also experience significant mass loss during the mass-transfer process (e.g., de Mink et al. 2007; Shao & Li 2016).

LB-1 is located at a distance of $\sim 2\text{--}4$ kpc and has a V-band apparent magnitude of ~ 12 mag (Liu et al. 2019), which is much fainter than other observed Be–He binaries. Whether LB-1 is a black hole binary or a Be star binary will considerably influence the strategy of black hole search with optical observations. It is also noted that, although there are a few theoretical investigations on the formation of specific Be–He binaries, a systematic work on the whole population is still lacking. In this paper, we explore the possible properties of the Be–He systems in the Milky Way. Our main goal is to obtain the predicted number and the parameter distribution of the Be–He binary population, by taking into account different mass-transfer models (efficiencies) during the progenitor binary evolution. The remainder of this paper is organized as follows. In Section 2, we present the binary population synthesis (BPS, see Han et al. 2020, for a review) method. We present the calculated results in Section 3. We briefly discuss their implications in Section 4 and conclude in Section 5.

2. METHOD

We employ the *BSE* code originally developed by Hurley et al. (2002) to deal with the formation and evolution of Be–He binaries. Significant modification in this code has been made by Shao & Li (2014) to deal with the mass-transfer stability and common envelope evolution. This code makes use of a series of fitting formulae (Hurley et al. 2000) to describe the structure of single stars as they evolve as a function of the stellar mass and age, so it can rapidly compute the evolution of millions of binary systems. Modelling the evolution of a binary system involves detailed treatments of stellar winds, tidal interactions, and mass and angular momentum transfer.

Starting from a primordial binary with two zero-age main sequence stars, the primary star first evolves to fill its Roche lobe and supplies its envelope material to the secondary star. Mass accretion onto the secondary star causes it to expand and spin up. The expanded size of the secondary star is strongly dependent on the mass accretion rate (e.g., Neo et al. 1977). Usually rapid mass accretion can drive the secondary star to get out of thermal equilibrium and significantly expand, leading to the formation of a contact binary if the secondary star has also filled its own Roche lobe (Nelson & Eggleton 2001). Following Shao & Li (2014) we build three mass transfer models. In Model I, the mass accretion rate onto the secondary is assumed to be the mass-transfer rate multiplied by a factor of $(1 - \Omega/\Omega_{\text{cr}})$, where Ω is the angular velocity of the secondary star and Ω_{cr} is its critical value (see also Stancliffe & Eldridge 2009). By simulating the evolution

of massive binaries under the assumption of this model, Shao & Li (2016) pointed out that the averaged mass-transfer efficiencies decrease from ~ 0.7 to ~ 0.1 with increasing binary orbital periods. In Model II, it is assumed that the secondary star accretes half of the transferred matter with a constant mass-transfer efficiency of 0.5. In Model III, the mass accretion rate is assumed to be limited by a factor of $\min[10(\tau_{\dot{M}}/\tau_{\text{KH}}), 1]$, where $\tau_{\dot{M}}$ is the mass-transfer timescale and τ_{KH} is the thermal timescale of the secondary star (Hurley et al. 2002). Generally the mass-transfer process in Model III is near-conservative (Shao & Li 2014), and we demonstrate that the averaged mass-transfer efficiencies for almost all binaries are higher than 0.95 after dealing with the data of our BPS calculations. In all the cases, the escaped material from the binary system is assumed to carry away the specific orbital angular momentum of the secondary star. As a consequence, the maximal initial mass ratios of the primary to the secondary star for avoiding the contact phase can reach as high as ~ 6 in Model I, and drops to ~ 2.5 and ~ 2.2 in Model II and III, respectively (Shao & Li 2014). We assume that all contact binaries evolve into a common-envelope phase.

We include the effect of stellar winds, tides and mass exchange on the rotational velocity of the secondary star (see e.g., de Mink et al. 2013). The internal rotational profile of the secondary star is approximated to be rigid rotation, which is a reasonable approximation for the secondary star residing at the main-sequence stage (e.g., Maeder & Meynet 2005; Brott et al. 2011). When the mass transfer occurs via Roche lobe overflow, the rotational evolution of the secondary star is mainly controlled by the competition between the spin-down effect due to tidal interactions and the spin-up effect due to mass and angular momentum accretion. We follow Hurley et al. (2002) to treat the spin-orbit coupling between binary components due to tidal interactions. During the mass-transfer process, the transferring matter may either form an accretion disk around the secondary star or directly impact on its surface, depending on the minimum distance R_{min} between the mass stream and the secondary star (Lubow & Shu 1975) compared with the radius R_s of the secondary star. If $R_{\text{min}} > R_s$, the mass stream is assumed to collide with itself after which the viscous process leads to the formation of an accretion disk. It is assumed that the secondary star accretes matter from the inner edge of the disk with the specific angular momentum of $\sqrt{GM_s R_s}$, where G is the gravitational constant and M_s is the secondary mass. Otherwise, the matter stream impacts directly on the surface of the secondary star and the specific angular momentum of the impact stream is estimated to be $\sqrt{1.7GM_s R_{\text{min}}}$.

According to the observational characteristics of Be stars, we identify them as the main-sequence stars with masses of $3 - 23M_{\odot}$ (spectral types of A0–O9) and rotational velocities exceeding 80% of their Keplerian limits (Slettebak 1982; Negueruela 1998; Porter & Rivinius 2003). As shown by Shao & Li (2014), the formation of Be stars in binary systems does not favour a common-envelope phase during the primordial evolution, so we only consider the case of stable mass transfer via Roche lobe overflow to produce Be stars in our calculations. Evolved from the primordial binaries, the formation of Be–He binaries usually experiences either Case

A or Case B mass transfer (Kippenhahn & Weigert 1967; Paczyński 1967). For relatively close primordial binaries, mass transfer starts when the primary stars are still on the main-sequence phase with a burning hydrogen core (Case A mass transfer). The primary stars will experience a rapid contraction after the depletion of fuel in their convective cores, leading to a temporary detachment of the binary systems. When the primary stars expand due to shell hydrogen burning and fill their Roche lobes again, Case AB mass transfer takes place. For relatively wide primordial binaries, the primary stars are on the shell hydrogen burning phase when mass transfer begins (Case B mass transfer). We follow Hurley et al. (2002) to age the primary stars and rejuvenate the secondary stars due to mass exchange. After mass transfer, the primary stars leave stripped-down, bare He-burning stellar cores that are referred to He stars in the present context.

We have evolved a large number ($\sim 10^7$) of binary systems in each model, by setting a grid of initial parameters as follows. The primary masses M_1 vary in the range of $1 - 60M_\odot$, the secondary masses M_2 in the range of $0.1 - 60M_\odot$, and the orbital separations a in the range of $3 - 10^4R_\odot$. For the primary stars, less massive ($\lesssim 2M_\odot$) ones can only develop degenerate He cores (Hurley et al. 2000), and more massive ($> 60M_\odot$) ones are extremely rare due to the initial mass function (IMF). For the secondary stars, only the systems with $M_2 < M_1$ are evolved. Each parameter χ is logarithmically spaced with the n_χ grid points, thus

$$\delta \ln \chi = \frac{1}{n_\chi - 1} (\ln \chi_{\max} - \ln \chi_{\min}). \quad (1)$$

If a specific binary i evolves through a phase that is identified as a Be–He binary, then the system can contribute the population with a rate

$$R_i = \left(\frac{f_b}{f_s + 2f_b} \right) \left(\frac{S}{M_*} \right) \Phi(\ln M_{1i}) \varphi(\ln M_{2i}) \Psi(\ln a_i) \delta \ln M_1 \delta \ln M_2 \delta \ln a, \quad (2)$$

where f_s and f_b are respectively the fractions of single stars and binary (including multiple) systems among all stars, so the relation of $f_s + f_b = 1$ is always satisfied. Here S is the star formation rate of the Milky Way and $M_* \sim 0.5M_\odot$ is the average mass of all stars. Considering the star formation history of the Milky Way, we use a constant star formation rate of $S = 3M_\odot \text{ yr}^{-1}$ over the past 10 Gyr period (Smith et al. 1978; Diehl et al. 2006; Robitaille & Whitney 2010). $\Phi(\ln M_{1i})$, $\varphi(\ln M_{2i})$ and $\Psi(\ln a_i)$ are the normalized functions to weight the contribution of the specific binary with logarithmic parameters of $\ln M_{1i}$, $\ln M_{2i}$ and $\ln a_i$, respectively. Since the initial parameters of primordial binaries cover rather wide ranges, all input values and the corresponding distribution functions are taken in the logarithmic forms. A more detailed description can be found in the method section of Hurley et al. (2002). The masses of the primary stars follow the Kroupa et al. (1993) IMF,

$$\xi(M_1) = \begin{cases} 0 & M_1 \leq 0.1M_\odot \\ a_1 M_1^{-1.3} & 0.1M_\odot < M_1 \leq 0.5M_\odot \\ a_2 M_1^{-2.2} & 0.5M_\odot < M_1 \leq 1.0M_\odot \\ a_2 M_1^{-2.7} & 1.0M_\odot < M_1 < \infty. \end{cases} \quad (3)$$

where $a_1 = 0.29056$ and $a_2 = 0.15571$ are the normalized parameters. Then

$$\Phi(\ln M_1) = M_1 \xi(M_1). \quad (4)$$

We assume that the secondary masses M_2 obey a flat distribution between 0 and M_1 (Kobulnicky & Fryer 2007), thus giving

$$\varphi(\ln M_2) = \frac{M_2}{M_1}. \quad (5)$$

The distribution of the initial orbital separations a is assumed to be logarithmically uniform between 3 and 10^4R_\odot (Abt 1983), thus we obtain

$$\Psi(\ln a) = k = \text{const.} \quad (6)$$

The normalization of this distribution gives $k = 0.12328$. We assume that all binaries initially have circular orbits, as the outcome of the interactions of systems with the same semilatus rectum is almost independent of eccentricity (Hurley et al. 2002). All stars are assumed to be initially in binaries¹. The initial metallicity of stars is taken to be $Z = 0.02$. The Galactic thin disk is an active site for ongoing star formation, which dominates the formation of relatively massive binaries that we are working with. Observations of HII regions via radio continuum emission indicate that ongoing star formation occurs with a nearly uniform efficiency over the Galactic thin disk (Kennicutt & Evans 2012, and references therein). We simply assume that the Galactic thin disk is infinitesimally thin and the recent star-formation rate has a uniform distribution over the disk. We adopt the distance of the Sun with respect to the Galactic center to be 8 kpc (Feast & Whitelock 1997). The Be–He binaries are assumed to locate at their birth places without considerable movement, considering the relatively small velocities and short lifetimes of massive binaries.

For the detection of Be–He binaries, we can predict the possible distributions of some observational parameters including the apparent magnitude and the radial velocity semi-amplitude of the binary components. Based on stellar luminosity L , effective temperature T_{eff} and surface gravity g , we edit a subroutine in the code to yield the V-band absolute magnitude M_V . Under the scheme of Vega magnitude system, Girardi et al. (2002) tabulated the bolometric corrections with a grid of T_{eff} and $\log g$, which were obtained from the combination of the real atmospheric spectra (Fluks et al. 1994; Castelli et al. 1997; Allard et al. 2000) and the Planck black-body spectra (for very hot stars). In our calculations, the bolometric correction for a specific star is given by a linear interpolation in the existing grid. By considering the interstellar extinction A_V in the V band, the apparent magnitude m_V can be given as

$$m_V = M_V + 5 \left(2 + \log \left(\frac{D}{1 \text{ kpc}} \right) \right) + A_V(D), \quad (7)$$

where D is the distance of the binary system from the Sun. Since the average extinction of the Galactic disk is $\sim 1 \text{ mag kpc}^{-1}$ (Spitzer 1978), we adopt $A_V(D) = \frac{D}{1 \text{ kpc}}$.

¹ Observations show that most ($f_b \sim 0.6 - 0.9$) of OB stars are born as members of binary and multiple systems (Moe & Di Stefano 2017), this can reduce our calculated birthrate and expected number of Galactic Be–He binaries by a factor of less than 2.

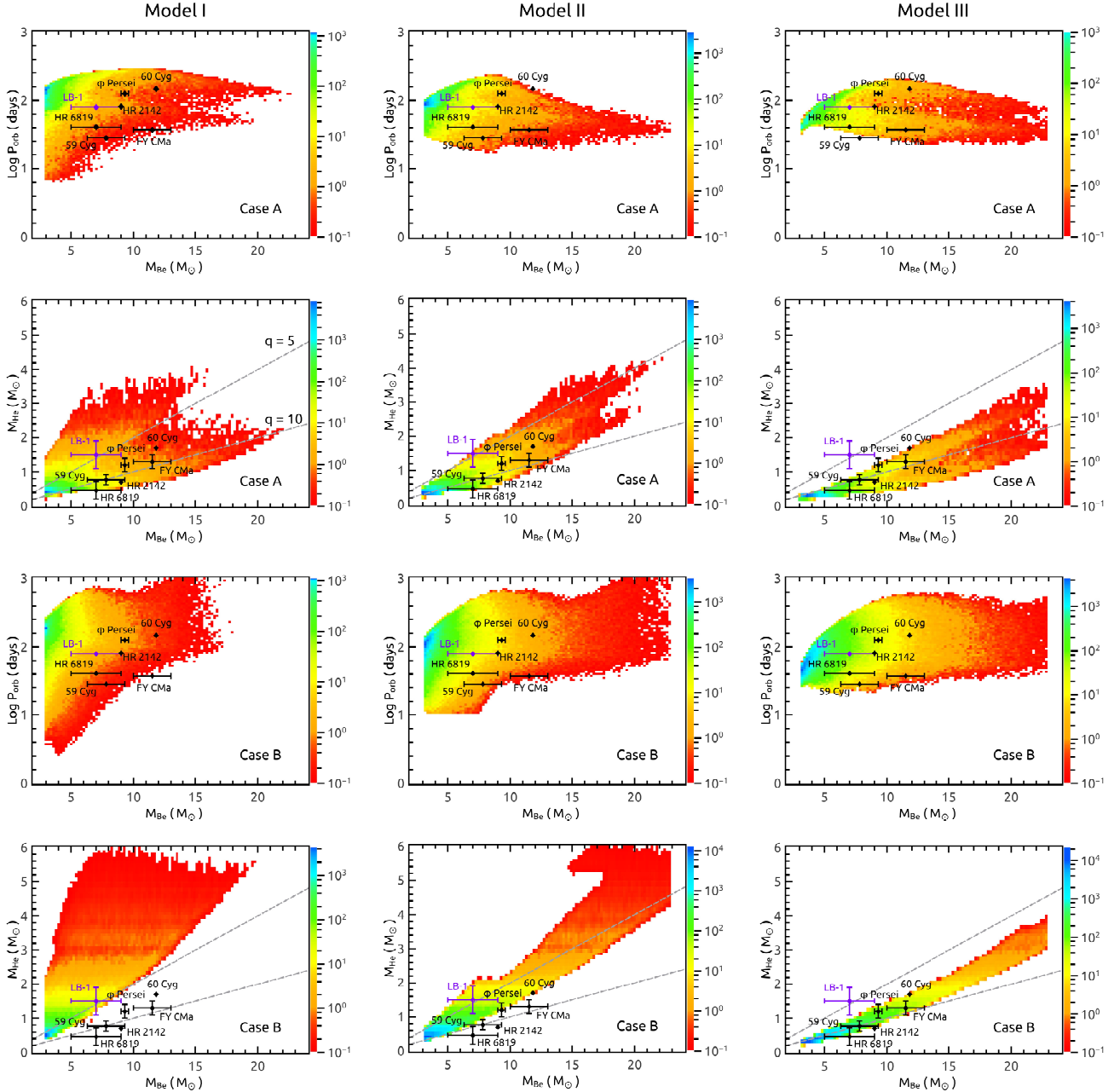


FIG. 1.— Calculated number distributions of Galactic Be–He binaries in the $M_{\text{Be}} - P_{\text{orb}}$ and $M_{\text{Be}} - M_{\text{He}}$ planes under the assumption of Models I–III (from left to right). The top and bottom six panels correspond to the evolution of the progenitor systems experienced the process of Case A and Case B mass transfer, respectively. The positions of suggested Be–He systems are plotted with solid diamonds—the purple one corresponds to LB-1 while the black ones correspond to other binaries. For 60 Cyg and HR 2142 without error bars in mass, the Be-star masses are crudely estimated from their spectral classifications (Koubský et al. 2000; Peters et al. 2016). The colors in each pixel are scaled according to the corresponding numbers, only the systems with numbers larger than 0.1 are plotted. The two dashed lines correspond to mass ratios $q (= M_{\text{Be}}/M_{\text{He}})$ equal to 5 and 10 for comparison.

To estimate the radial velocity semi-amplitude K , the orbital inclination of Be–He binaries is assumed to distribute uniformly between 0 and 2π . From the BPS outcomes, we select all Be–He binaries and record relevant parameters at each of the evolutionary steps. The corresponding number of a specific type of binary can be evaluated by multiplying its birthrate with the timestep.

3. RESULTS

Figure 1 shows the calculated number distributions of Galactic Be–He binaries in the $M_{\text{Be}} - P_{\text{orb}}$ and

$M_{\text{Be}} - M_{\text{He}}$ planes under the assumption of Models I–III. The top and bottom six panels correspond to the evolution of the progenitor systems experienced the process of Case A and Case B mass transfer, respectively. Each panel includes a 100×100 matrix element for the corresponding binary parameters. The color in each pixel reflects the number of Be–He binaries in the corresponding matrix element by accumulating the product of the birthrates of the binary systems passing through it with the timespan. The solid diamonds mark the positions of suggested Be–He binaries and the purple one corre-

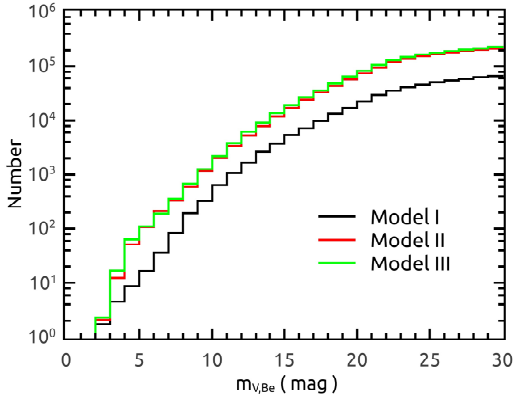


FIG. 2.— Accumulated number distributions of Galactic Be–He binaries as a function of the V-band apparent magnitude of the Be stars. The three coloured curves correspond to Models I–III.

sponds to LB-1 if it is a Be–He binary. In Model II, there is a jump at $M_{\text{He}} \sim 2 - 5 M_{\odot}$ in the $M_{\text{Be}} - M_{\text{He}}$ plane for the systems that experienced Case B mass transfer. The reason is that the mass-transfer stability during the primordial binary evolution is sensitive to the orbital periods and the mass ratios, leading to the parameter spaces for stable mass transfer be irregular and odd (see Section 2.2 of Shao & Li 2014). Our calculations show that the orbital periods of the binary systems mainly distribute in a range of ~ 10 to a few 100 days. Although the mass-transfer efficiencies are significantly different in the three models, they all predict that the Be–He binaries tend to have light components due to the IMF. When the mass transfer occurs at the main-sequence stage, the Case A evolution tends to produce the binaries with relatively large mass ratios $q (= M_{\text{Be}}/M_{\text{He}})$, which can extend to $\gtrsim 5 - 10$. Our calculations show that slightly more ($\sim 50\%$ in Model I, $\sim 70\%$ in Model II, and $\sim 80\%$ in Model III) Be–He binaries are formed via Case B evolution. In Model III we can well reproduce the observed sample except LB-1, while in Models I and II the formation of these systems favours Case A evolution. We emphasize that near-conservative mass transfer (i.e., Model III) is unable to form LB-1 with $q \sim 5$ (Shenar et al. 2020), because the Be star has accreted too much mass from the progenitor of the He star.

Fig. 2 presents the cumulative number distributions of Galactic Be–He binaries as a function of the V-band apparent magnitude of the Be stars in Models I–III. We predict that the total number of Be–He binaries in the Milky Way is $\sim 8 \times 10^4$ in Model I, and increases to $\sim 2.3 \times 10^5$ in Model II and to $\sim 2.8 \times 10^5$ in Model III (see also Shao & Li 2014). This is because more efficient mass transfer can decrease the lower limit of the primary mass when the minimal mass of Be stars is fixed to be $3M_{\odot}$, thus increasing the formation rate of Be–He binaries due to the IMF. Considering that LB-1 has the V-band apparent magnitude of ~ 12 (Liu et al. 2019), we estimate that there are $\sim 1100 - 3800$ Be–He systems with V-band apparent magnitudes brighter than LB-1. Note that the Be stars are greatly brighter than the He stars in the V band for most of Galactic Be–He binaries (see Fig. 5), since the He stars are much hotter and shine mostly in the UV band. It is expected that a part of mass gainers may spin down and appear as reg-

ular B-type stars due to angular momentum losses via tides and stellar winds. Since the majority of Galactic Be–He systems are expected to contain a late-type Be star, the stellar winds are too weak to spin down the Be stars which are able to keep the Be phenomenon in the whole main-sequence stage. The rotation of the mass gainers in close binaries tends to synchronize with the orbital motion due to tidal interactions. Since significant orbital angular momentum loss via the escaped material during the evolution, Model I can produce more binaries with relatively short periods. We find that the post-mass transfer binaries with a regular B-type star around a He star are numerous and we find the most in Model I, estimating them to be $\sim 1.1 \times 10^4$ in the Galaxy, while in Model II and III we estimate them to be $\sim 2.1 \times 10^3$ and $\sim 1.1 \times 10^3$, respectively. It is indicated that the mass gainers in the majority ($\gtrsim 90\%$) of post-mass transfer binaries can remain to be Be stars in all our models. There is a caveat that many binaries with a regular B-type star and a He star may be created via the ejection of a common envelope, which is not involved in our calculations.

Fig. 3 shows the histogram number distributions of the calculated Be–He binaries as a function of the Be-star mass, the He-star mass, the orbital period, and the radial velocity semi-amplitude of the Be star in Models I–III (from top to bottom). The black curves correspond to all Be–He systems, while the red curves correspond to the Be–He systems with Be stars brighter than 12 mag. We see that the shapes of the number distribution of Be–He binaries in these two cases are similar. The mass distribution of the Be stars has a peak at $\sim 3M_{\odot}$, and the number of the binary systems rapidly decreases with increasing Be-star mass. A similar case can be found for the He-star mass distribution but with a peak $\sim 0.3 - 0.6M_{\odot}$. The peak of the orbital period distribution shifts from ~ 160 days to ~ 80 days with gradually increasing mass-transfer efficiencies from Model I to Model III. In all cases, the radial velocity semi-amplitudes of the Be star distribute in the range of $\lesssim 100 \text{ km s}^{-1}$ with a peak near 8 km s^{-1} .

In Fig. 4 we depict predicted number distributions of Galactic Be–He binaries in the parameter space of Be-star apparent magnitude vs. binary distance for Models I–III. We can see that the binaries with Be stars brighter than 12 mag can be detected within the distances of $\lesssim 4$ kpc. A large number of Be–He binaries are expected to be located at a distance of $\sim 5 - 10$ kpc, in which the Be stars have the V-band apparent magnitudes of $\sim 20 - 25$.

4. OBSERVATIONAL CONSEQUENCES

The detection of Be–He binaries is subject to serious observational biases (Götberg et al. 2017; Schootemeijer et al. 2018). Most of systems appear to be single stars. Even for the observed Be–He binaries, part of them were suggested to have atypical parameters. For example, Schootemeijer et al. (2018) pointed out that the stripped He stars in φ Persei and 59 Cyg are remarkably bright for their current masses. It was explained that these stripped stars reside in the He-shell rather than He-core burning phase. The detection of such short-lived binaries implies that a large fraction of the systems containing a less-evolved He star may remain undetected. Also, if LB-1 is a Be–He binary, its properties seem to deviate from the typical ones. The estimated parameters

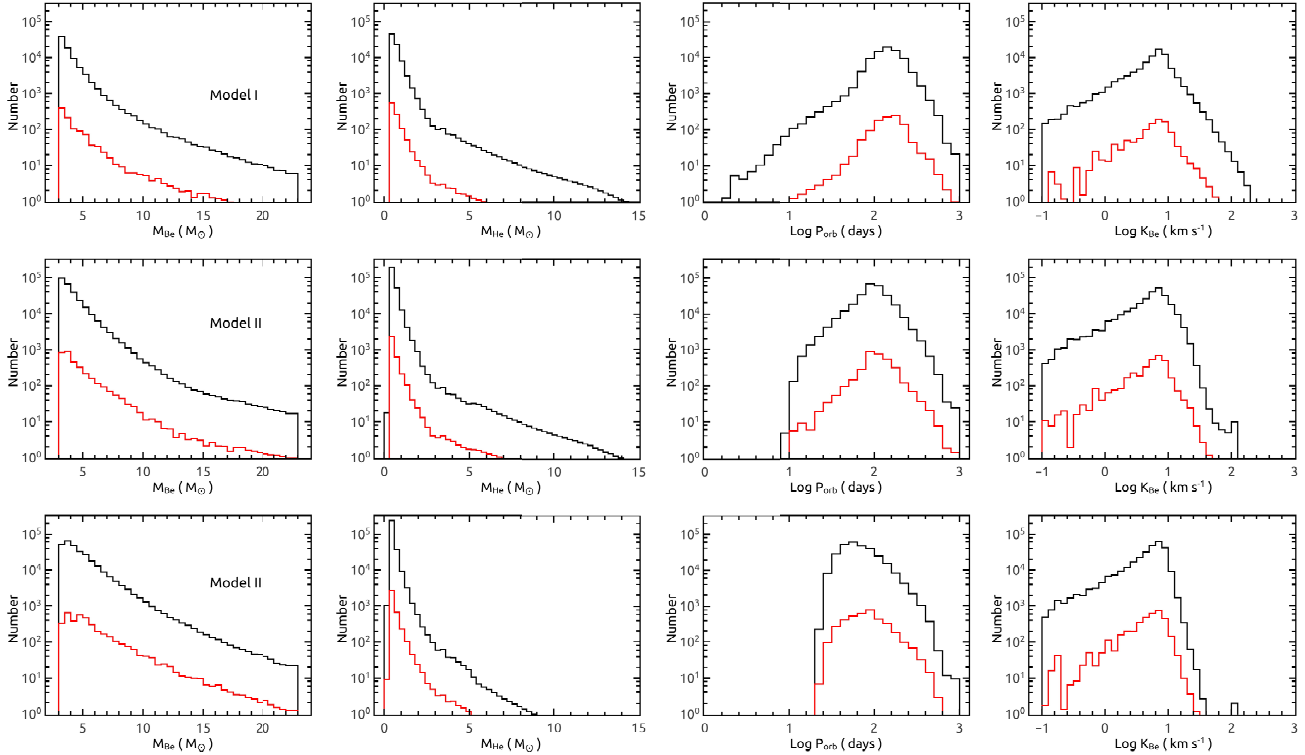


FIG. 3.— Calculated number distributions of Galactic Be–He binaries as a function of the Be-star mass M_{Be} , the He-star mass M_{He} , the orbital period P_{orb} , and the radial velocity semi-amplitude K_{Be} of the Be star in Models I–III (from top to bottom). The black curves correspond to all Be–He binaries, and the red curves correspond to the systems with Be stars brighter than 12 mag in the V band.

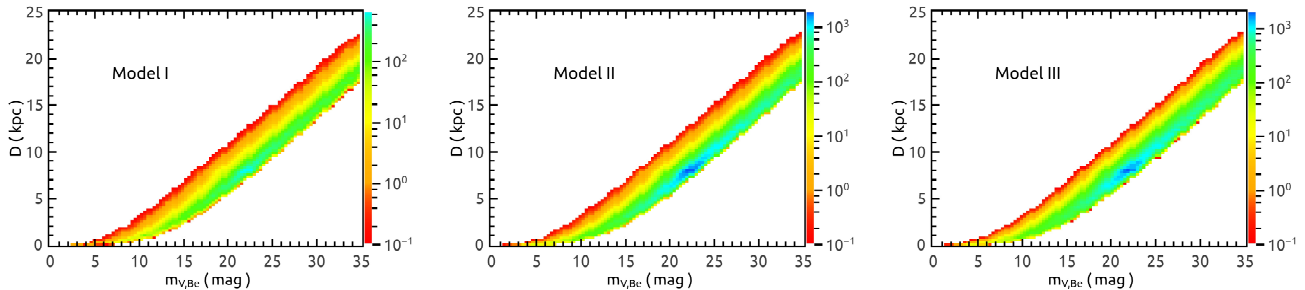


FIG. 4.— Calculated number distributions of Galactic Be–He binaries in the parameter space of Be-star apparent magnitude vs. binary distance. The three panels correspond to Models I–III. The colors in each pixel are scaled according to the corresponding numbers, only the systems with numbers larger than 0.1 are plotted.

for the components of LB-1 (Shenar et al. 2020) indicate that the stripped star is slightly colder than the Be star, thus both components can significantly contribute to the optical emission. The relatively cold stripped star implies that it is thermally unstable, most likely contracting towards the He main sequence (Shenar et al. 2020). This evolutionary phase can last for a duration about 1 – 2 orders of magnitude shorter than the lifetime of a He star (Eldridge et al. 2020), indicating again that a large number of Be–He binaries should exist but be hidden.

In Fig. 5, we present the calculated number distributions of all Galactic Be–He binaries in the parameter space of the absolute magnitudes of both components. The solid triangles mark the positions of observed binaries, for which the absolute magnitudes are estimated from the corresponding stellar parameters (data taken from Schootemeijer et al. 2018; Shenar et al. 2020; Bo-

densteiner et al. 2020b). It is obvious that the calculated Be–He binaries mainly distribute in two regions with $(M_{V,\text{Be}}, M_{V,\text{He}})$ clustering around $(-1 \text{ mag}, 6 \text{ mag})$ and $(-1 \text{ mag}, 1 \text{ mag})$. This two-region distribution is just dependent on whether the He star is in the contraction phase with a bloated envelope². Note that the He stars during the He-shell burning phase can also develop a bloated envelope and are relatively bright in the V band, the systems with such a He star tend to cover a large region in the $M_{V,\text{Be}} - M_{V,\text{He}}$ plane. We predict that the numbers of the binary systems with a contracting (expanding) He star are about 1.5×10^4 (4.9×10^3)

² In order to identify the binaries with a stripped star being in the contraction phase (labelled as a giant star in the BSE code), we pick out all detached Be-star binaries with either a giant star or a He star companion. After using a criterion of $M_{\text{He}} < 0.6M_1$, we find that the stripped star continuously evolves from a giant star to a naked He star for a specific binary.

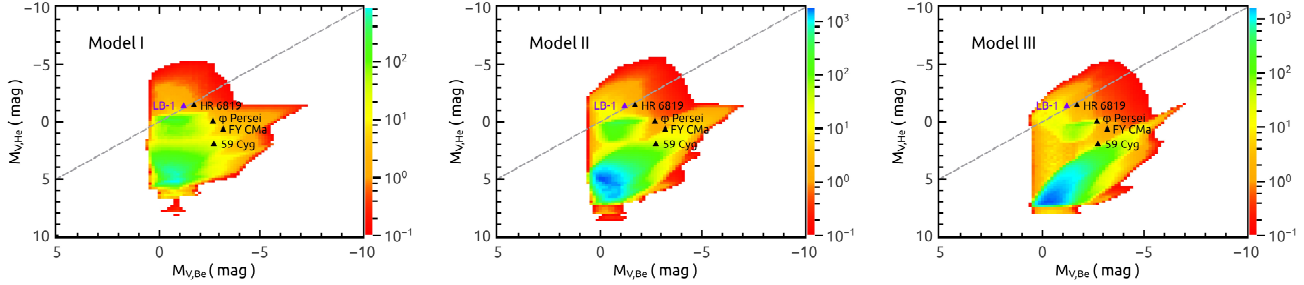


FIG. 5.— Calculated number distributions of all Galactic Be–He binaries in the $M_{V,Be} - M_{V,He}$ plane under the assumption of Models I–III (from left to right). The colors in each pixel are scaled according to the corresponding numbers, only the systems with numbers larger than 0.1 are plotted. The positions of suggested Be–He systems are plotted with solid triangles—the purple one corresponds to LB-1 while the black ones correspond to other binaries. The dashed line in each panel corresponds to $M_{V,Be} = M_{V,He}$.

in Model I, 1.7×10^4 (1.2×10^4) in Model II, and 8×10^3 (2.7×10^3) in Model III. Compared to the total number of Galactic Be–He systems, we can estimate that about 4%–20% of all binaries harbour a bloated He star. However, there are only $\sim 1\%$ of the Galactic Be–He binaries with He stars brighter than Be stars in the V band.

5. CONCLUSION

We use the BPS method to simulate the potential population of Be–He binaries in the Milky Way. Since the mass-transfer process during the progenitor system evolution is still uncertain, we consider three models to deal with the binary evolution. Comparison of the parameter distributions of the calculated Be–He binaries with the inferred properties of LB-1 indicates that the progenitor system of LB-1 very likely has experienced a non-conservative mass transfer, if it is a Be–He system. Combining with other formation channel(s) of other observed binaries such as φ Persei (Pols 2007; Schootemeijer et al.

2018), this indicates that the mass-transfer processes in massive binary evolution are complicated, depending on the detailed characteristics of the binaries. We estimate that the total number of Galactic Be–He binaries is of the order 10^5 , and $\sim 1100 - 3800$ of them are expected to have the V-band apparent magnitudes brighter than LB-1. If assuming a few percent of such Be–He binaries have a stripped star being in the contraction phase, there remain at least tens of systems similar to LB-1 to be discovered.

We thank the anonymous referee for constructive suggestions that helped improve this paper. This work was supported by the Natural Science Foundation of China (Nos. 11973026 and 11773015), the Project U1838201 supported by NSFC and CAS, and the National Program on Key Research and Development Project (Grant No. 2016YFA0400803).

REFERENCES

- Abdul-Masih, M., Banyard, G., Bodensteiner, J. et al. 2020, *Nature*, 508, 11
- Abt, H. A. 1983, *ARA&A*, 21, 343
- Allard, F., Hauschildt, P. H., Alexander, D. R., et al. 2000, *ASPC*, 212, 127
- Belczynski, K., Bulik, T., Fryer, C. L., et al. 2010, *ApJ*, 714, 1217
- Belczynski, K., Hirschi, R., Kaiser, E. A. et al. 2020, *ApJ*, 890, 113
- Bodensteiner, J., Shenar, T., & Sana, H. 2020a, *A&A*, 641, 42
- Bodensteiner, J., Shenar, T., Mahy, L. et al. 2020b, *A&A*, 641, 43
- Brott, I., de Mink, S. E., Cantiello, M., et al. 2011, *A&A*, 530, 115
- Castelli, F., Gratton, R. G., & Kurucz, R. L. 1997, *A&A*, 318, 841
- de Mink, S. E., Pols, O. R., & Hilditch, R. W. 2007, *A&A*, 467, 1181
- de Mink, S. E., Langer, N., Izzard, R. G., Sana, H., & de Koter, A. 2013, *ApJ*, 764, 166
- Diehl, R., Halloin, H., Kretschmer, K., et al. 2006, *Nature*, 439, 45
- Ekström, S., Meynet, G., Maeder, A., & Barblan, F. 2008, *A&A*, 478, 467
- El-Badry, K. & Quataert, E. 2020, *MNRAS*, 493, L22
- Eldridge, J. J., Stanway, E. R., Breivik, K. et al. 2020, *MNRAS*, 495, 2786
- Farmer, R., Renzo, M., de Mink, S. E., Marchant, P., Justham, S. 2019, *ApJ*, 887, 53
- Feast, M., & Whitelock, P. 1997, *MNRAS*, 291, 683
- Fluks, M. A., Plez, B., The, P. S., et al. 1994, *A&AS*, 105, 311
- Giesers, B., Dreizler, S., Husser, T.-O., et al. 2018, *MNRAS*, 475, L15
- Girardi, L., Bertelli, G., Bressan, A. et al. 2002, *A&A*, 391, 195
- Götberg, Y., de Mink, S. E., & Groh, J. H. 2017, *A&A*, 608, A11
- Groh, J. H., Farrell, E., Meynet, G. et al. 2019, *ApJ*, 900, 98
- Han, Z.-W., Ge, H.-W., Chen, X.-F., & Chen, H.-L. 2020, *RAA*, 20, 16
- Hastings, B., Wang, C., & Langer, N. 2020, *A&A*, 633, 165
- Huang, W., Gies, D. R., & McSwain, M. V. 2010, *ApJ*, 722, 605
- Hurley, J. R., Pols, O. R., & Tout, C. A. 2000, *MNRAS*, 315, 543
- Hurley, J. R., Tout, C. A., & Pols, O. R. 2002, *MNRAS*, 329, 897
- Irrgang, A., Geier, S., Kreuzer, S. et al. 2020, *A&A*, 633, L5
- Kennicutt, R. C., & Evans, N. J. 2012, *ARA&A*, 50, 531
- Kippenhahn, R., & Weigert, A. 1967, *ZA*, 65, 251
- Kobulnicky, H. A., & Fryer, C. L. 2007, *ApJ*, 670, 747
- Kobulnicky, H. A., Kiminki, D. C., Lundquist, M. J., et al. 2014, *ApJS*, 213, 34
- Koubský, P., Harmanec, P., Hubert, A. M. et al. 2000, *A&A*, 356, 913
- Koubský, P., Kotková, L., Votruba, V. et al. 2012, *A&A*, 545, 121
- Kroupa, P., Tout, C. A., & Gilmore, G. 1993, *MNRAS*, 262, 545
- Langer, N., Baade, D., Bodensteiner, J. et al. 2020, *A&A*, 633, 40
- Liu, J., Zhang, H., Howard, A. et al. 2019, *Nature*, 575, 618
- Liu, J., Soria, R., Zheng, Z. et al. 2020, *Nature*, 580, 16
- Lubow, S. H., & Shu, F. H. 1975, *ApJ*, 198, 383
- Maeder, A., & Meynet, G. 2005, *A&A*, 440, 1041
- McSwain, M. V., & Gies, D. R. 2005, *ApJS*, 161, 118
- Moe, M., & Di Stefano, R., 2017, *ApJS*, 230, 15
- Mourard, D., Monnier, J. D., Meilland, A., et al. 2015, *A&A*, 577, A51
- Neguera, I. 1998, *A&A*, 338, 505
- Nelson, C. A. & Eggleton, P. P. 2001, *ApJ*, 552, 664
- Neo, S., Miyaji, S., Nomoto, K., & Sugimoto, D. 1977, *PASJ*, 29, 249
- Paczyński, B. 1967, *AcA*, 17, 355

- Peters, G. J., Gies, D. R., Grundstrom, E. D., & McSwain, M. V. 2008, *ApJ*, 686, 1280
- Peters, G. J., Pewett, T. D., Gies, D. R., Touhami, Y. N., & Grundstrom, E. D. 2013, *ApJ*, 765, 2
- Peters, G. J., Wang, L., Gies, D. R., & Grundstrom, E. D. 2016, *ApJ*, 828, 47
- Pols, O. R., Coté, J., Waters, L. B. F. M., & Heise, J. 1991, *A&A*, 241, 419
- Pols, O. R. 2007, *ASP Conf. Ser.*, 367, 387
- Porter, J. M., & Rivinius, T. 2003, *PASP*, 115, 1153
- Rappaport, S., & van den Heuvel, E. 1982, in *IAU Symp. 92, Be Stars*, ed. M. Jaschek & H. G. Groth (Dordrecht: Reidel), 327
- Rivinius, Th., Baade, D., Hadrava, P., Heida, M., & Klement, R. 2020, *A&A*, 637, 3
- Robitaille, T. P., & Whitney, B. A. 2010, *ApJL*, 710, L11
- Sana, H., de Mink, S. E., de Koter, A., et al. 2012, *Science*, 337, 444
- Schootemeijer, A., Góotberg, Y., de Mink, S. E., Gies, D., & Zapartas, E. 2018, *A&A*, 615, 30
- Smith, L. F., Biermann, P., & Mezger, P. G. 1978, *A&A*, 66, 65
- Shao, Y., & Li, X.-D. 2014, *ApJ*, 796, 37
- Shao, Y., & Li, X.-D. 2016, *ApJ*, 833, 108
- Shenar, T., Bodensteiner, J., Abdul-Masih, M. et al. 2020, *A&A*, 639, L6
- Simón-Díaz, S., Maíz Apellániz, J., Lennon, D. J. et al. 2020, *A&A*, 634, L7
- Slettebak, A. 1982, *ApJS*, 50, 55
- Spitzer, L. 1978, *Physical processes in the interstellar medium*, doi:10.1002/9783527617722
- Stancliffe, R. & Eldridge, J. 2009, *MNRAS*, 396, 1699
- Vanbeveren, D., De Loore, C., & Van Rensbergen, W. 1998, *A&ARv*, 9, 63
- Wang, L., Gies, D. R., & Peters, G. J. 2017, *ApJ*, 843, 60
- Wang, L., Gies, D. R., & Peters, G. J. 2018, *ApJ*, 853, 156